

## Design of a Frequency Reconfigurable Fabry-Pérot Cavity Antenna with Single Layer Partially Reflecting Surface

Peng Xie<sup>1</sup> and Guangming Wang<sup>2, \*</sup>

**Abstract**—A novel design of frequency reconfigurable Fabry-Pérot cavity antenna is presented. The superstrate of the antenna is a reconfigurable partially reflecting surface with PIN diodes on it. A dual-band patch antenna is used as the radiator of the antenna. Through changing the states of diodes, the partially reflecting surface can present different reflection phases, so the working frequency of the antenna can be tuned. The operation of frequency reconfiguration and the design method of the antenna are described exhaustively. A prototype antenna is fabricated and measured. The measured results show that the antenna can realize 13.1 dB gain at 4.6 GHz and 17.1 dB gain at 5.5 GHz with impedance bandwidths of 3.3% and 4.7%, respectively. Good agreement between the simulated and measured results is achieved, which proves the correctness of the design method. Besides, this method can also be used to design Fabry-Pérot cavity antenna working at other frequencies.

### 1. INTRODUCTION

Nowadays, leaky wave antennas have gained increased attention and have found wide applications in wireless communication systems. As one important branch of the leaky wave antennas, Fabry-Pérot cavity (FPC) antennas are preferred by scientists due to their high directive radiation [1, 2]. However, conventional FPC antennas usually have a narrow band due to the inherent limitations of the antenna structure. So most researches of the FPC antenna focuses on extending the working band [1–3]. Among them, broadband [4] and dual bands [5] are important improvement of the FPC antenna. Most of these antennas realize band improvement through using multilayer PRS. For example, a broadband FPC antenna is proposed in [6]. Two subwavelength cavities are formed by two artificial magnetic conductor (AMC) surfaces and ground plane. This structure makes the antenna achieve 8% bandwidth. In [7], a broadband FPC antenna based on multilayer partially reflective surfaces (PRS) is presented. Three-layer PRSs are introduced to enhance the band of the FPC antenna. The antenna realize around 20-dBi gain at the central operating frequency of 14.5 GHz with a bandwidth of about 15%. In [8], a dual- and wideband FPC antenna is presented. The dual-band operation is realized by using dissimilar double-square unit cells, while the bandwidth improvement is provided by two-layer PRSs with quasi-optimal reflection phase. The antenna realizes 3-dB gain bandwidths of 7% and 11% at two bands, respectively. However, these antennas suffer a common disadvantage of complex structure. There are some reports about dual-band FPC antenna with a single-layer superstrate in [9] and [10]. The superstrate of the antenna in [9] is a capacitive frequency selective surface (FSS) with square patch cell etched on a substrate. The proposed antenna can operate at the first and second resonant frequencies without altering the original antenna dimensions. However, it has a high frequency ratio (around 1.93), and it is difficulty to be changed. Ref. [10] presents a low profile dual-band resonant cavity antenna. The PRS of the antenna is formed by printing periodic array of metallic square loops and complementary

---

*Received 25 July 2017, Accepted 14 September 2017, Scheduled 29 September 2017*

\* Corresponding author: Guangming Wang (wgming01@sina.com).

<sup>1</sup> Air and Missile Defense College, Air Force Engineering University, Xi'an, China. <sup>2</sup> Department of Electromagnetic Field & Microwave Technique, Missile Institute of Air Force Engineering University, Sanyuan, China.

apertures on opposite sides of the dielectric material. This PRS makes the antenna achieve dual-band matching and gain enhancement.

In this paper, we propose a frequency reconfigurable FPC antenna with a single-layer PRS. First, a reconfigurable PRS which has tunable reflection phase is proposed. It is used as the superstrate of the FPC antenna. Then, a dual-band patch antenna is designed to work as the radiator of the FPC antenna. Through controlling the states of diodes on the PRS, the antenna can work at different frequencies. The operation of the frequency reconfiguration and the design method of the antenna are described exhaustively. The simulated and measured results show that the antenna keeps a high gain while shifting the working band. Moreover, the design method proposed in this paper can also be used to design FPC antenna working at other frequencies.

## 2. THEORY OF FPC ANTENNA

At the beginning, we analyze the working mechanism of the conventional FPC antenna. As shown in Fig. 1, a conventional FPC antenna consists of three important parts, namely PRS, ground plane and radiator. The PRS with special reflection phase  $\varphi$  is used to tune the working modes of the FPC antenna, which is set just above the radiator with a distance of  $h$ . According to the antenna theory [11], the FPC antenna can realize good radiation performance when the following equation is satisfied

$$\varphi + \pi - \frac{4\pi h}{\lambda} = -2N\pi, \quad N = 0, \pm 1, \pm 2 \dots \quad (1)$$

with  $\lambda$  being the wavelength in free space. We can extend the working modes of the FPC antenna by tuning the reflection phase of the PRS to obtain more solutions for Eq. (1). The most efficient way is to introduce active components in PRS design.

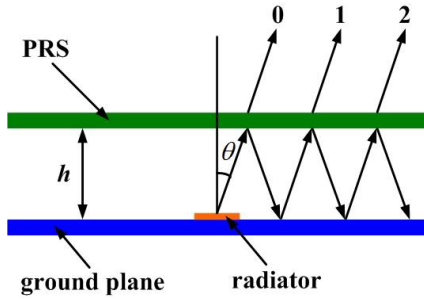


**Figure 1.** Schematic mode of the conventional FPC antenna.

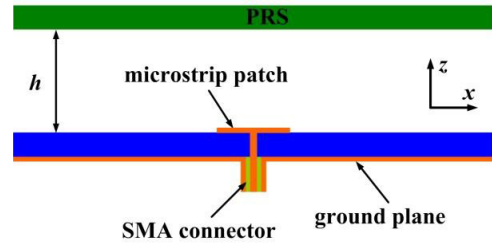


**Figure 2.** The structure of the FPC antenna.

## 3. DESIGN OF THE ANTENNA

We are going to design a frequency reconfigurable FPC antenna. The structure of the antenna is shown in Fig. 2. The height of the air gap is  $h_L$  when the antenna operates in low frequency band. Similarly, the height of the air gap is  $h_H$  when the antenna operates in high frequency band. These heights are defined as

$$h_L = \frac{(\varphi_L + \pi) \lambda_L}{4\pi} + \frac{N_L \lambda_L}{2} \quad (2a)$$

$$h_H = \frac{(\varphi_H + \pi) \lambda_H}{4\pi} + \frac{N_H \lambda_H}{2} \quad (2b)$$

Based on Eq. (2), when  $h_L = h_H$ , it can be expected that the antenna will realize frequency reconfiguration. In order to satisfy this condition, the reflection phase of the PRS should be tunable. Considering this, in the next section, we will design a reflection phase reconfigurable PRS.

### 3.1. Superstrate

To control the reflection phase of the PRS, we propose a novel reconfigurable unit. The topology of the unit is shown in Fig. 3. The unit is composed by a metal patch surrounded by a square ring, supported by a 1.6 mm-thick FR4 substrate with a permittivity of 4.4. The two gaps on the ring are used to insert two PIN diodes. The PIN diodes are controlled simultaneously, so the unit has two states, ON and OFF. The unit presents different reflection phases in different states. The width of the square patch  $w$  can influence the reflection phase of the unit. So we will search the reflection phase which is suitable for Eq. (1) through changing  $w$ . The reconfigurable PRS, shown in Fig. 4, is composed by  $10 \times 10$  units. On the surface, all the diodes are set along the same direction, so only a DC power is needed to bias all the diodes. The stub V connects to the anode of the DC source, and the stub Gnd connects the cathode of the DC source. The inductors (100 nH) are used to prevent the RF signal into the DC source. The PIN diodes used in the PRS are BAR50-03W which has a low forward bias resistance of  $1 \Omega$  and a low capacitance of 0.15 pF at reverse bias. In the simulation, a resistor of  $1 \Omega$  replaces the diode in the ON state while a parallel circuit, consisting of a capacitor of 0.15 pF and a resistor of  $10 \text{ k}\Omega$ , replaces the diode in the state OFF.

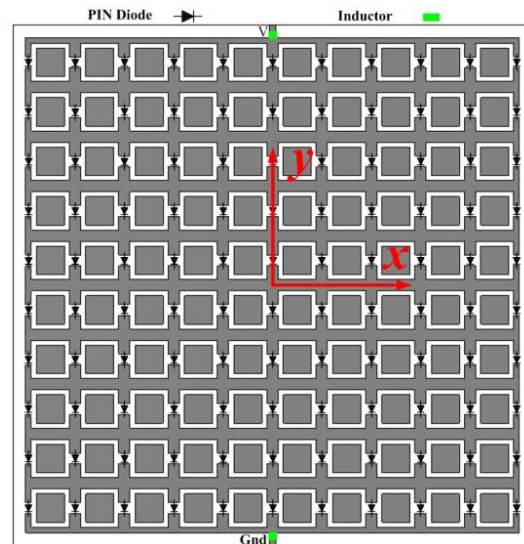
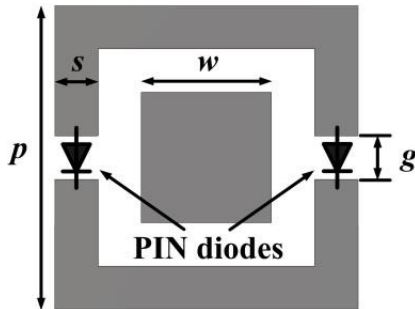


**Figure 3.** The reconfigurable unit ( $p = 14 \text{ mm}$ ,  $s = 1.6 \text{ mm}$ ,  $g = 2 \text{ mm}$ ). **Figure 4.** The configuration of the PRS.

### 3.2. Radiator

To realize the frequency reconfiguration of the FPC antenna, the radiator should have dual-band characteristics. The configuration of the patch antenna that we designed is shown in Fig. 5. The antenna is printed on a substrate of FR4 with a thickness of 1.6 mm and permittivity of 4.4. It has two patches connected by a stripline. The two patches have different lengths and widths, so they can resonate at different frequencies. The ground plane is on the bottom side of the substrate. An SMA connector is used to feed the antenna from the bottom of the substrate. The feeding point is on the stripline, and through tuning the position of the feeding point, the antenna can realize impedance matching. Four slits are etched on the patches beside the stripline. They are used to improve the impedance matching of the antenna. The antenna in this paper is designed to work at 4.6 GHz and 5.5 GHz. It is easy to change the working frequency of the patch antenna through changing the width and length of the two patches.

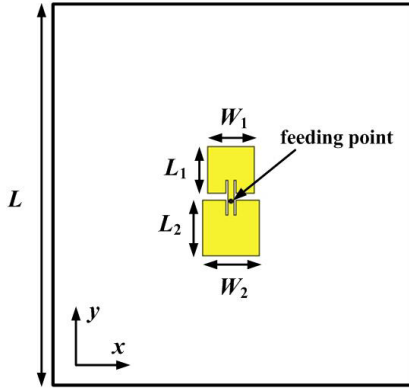


**Figure 5.** The geometry of the patch antenna. ( $L = 106$  mm,  $L_1 = 12.5$  mm,  $L_2 = 15.3$  mm,  $W_1 = 12.5$  mm,  $W_2 = 15.3$  mm).

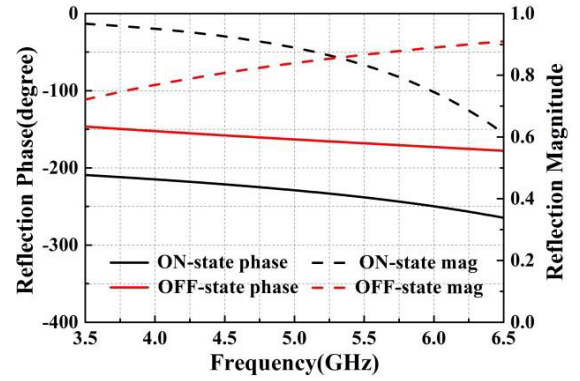


**Figure 6.** The simulation results of the unit.

### 3.3. Frequency Reconfiguration Operation

We simulated the reflection phase of the unit by CST. A periodic boundary is used in the simulation. The unit is simulated with an initial value of  $w = 7$  mm. The results are shown in Fig. 6. We can see that when the diodes are turned ON, the reflection phase of the unit will decrease. According to Eq. (1), when  $\varphi$  decreases, and  $h$  remains the same,  $\lambda$  should increase. So the antenna will work in low frequency band when the diodes are turned ON and in high frequency band when the diodes are turned OFF. Then, we simulate the reflection phase of the unit with the change of  $w$ . The results are shown in Fig. 7. We can see that the reflection phase decreases in both ON and OFF states with the increase of  $w$ . We regard the reflection phase of unit as the reflection phase of the PRS. In Eq. (2), in order to guarantee that FPC antenna works normally, the minimum of  $N$  is 1. In this condition, FPC antenna owns the smallest height (first order resonant length). The antenna is designed to work at 4.6 GHz and 5.5 GHz, so  $\lambda_L = 65.2$  mm and  $\lambda_H = 54.5$  mm. Then,  $h$  is determined by  $\varphi$ , and  $\varphi$  has relation with  $w$ . So we calculate the relationship between  $h$  and  $w$ . It is shown in Fig. 8. The black line comes from Eq. (2a) and the red line from Eq. (2b). We can find that the two lines have an intersection point. It is  $w = 8$  mm and  $h = 27.2$  mm. This illustrates that when  $h = 27.2$  mm and  $w = 8$  mm, the antenna will work at 4.6 GHz if the diodes are ON and at 5.5 GHz if the diodes are OFF. Thus, the antenna can realize frequency reconfiguration through controlling the state of the diodes. After optimization by the CST,  $h$  is set to 26.8 mm finally.

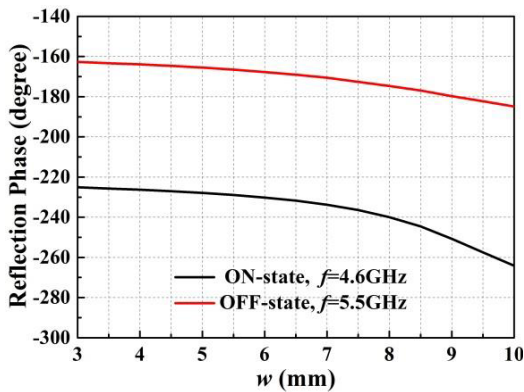


**Figure 7.** Variation of reflection phase with the  $w$ .

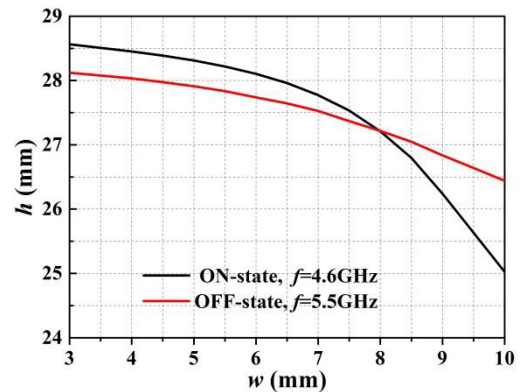


**Figure 8.** Calculated height of the air gap ( $h$ ).

### 3.4. Frequency Separation Ratio

The frequency separation ratio (high resonant frequency divided by low resonant frequency) is a significant performance of dual-band antennas. It is a great feature for dual-band antennas to have a small and tunable frequency separation ratio. The antenna proposed in this paper has a frequency separation ratio about 1.19. However, the biggest novelty of this paper is the new method to design frequency reconfigurable FPC antennas. This method can also be used to design FPC antenna working at other frequencies. Thus, the frequency separation ratio of the designed antenna is easy to be tuned.

## 4. SIMULATED AND MEASURED RESULTS

Photographs of the fabricated antenna are shown in Fig. 9. We measure  $S_{11}$  and radiation patterns of the antenna in both states. Fig. 10 shows simulated and measured  $S_{11}$  of the antenna. The measured results agree well with the simulated ones. When the diodes are ON, the working band of the antenna is 4.55–4.7 GHz (3.3%). When the diodes are OFF, the working band of the antenna is 5.37–5.63 GHz (4.7%). The measured center frequency of the antenna in ON state is a little higher than the simulated one. It may be caused by the fabrication errors.

Figure 11 shows the simulated and measured radiation patterns of the antenna. Fig. 11(a) is the patterns at 4.6 GHz in ON state and (b) is the patterns at 5.5 GHz in OFF state. Good agreement is obtained between the simulated and measured results. The antenna has broadside patterns in both states with a high gain. Besides, the 3-dB gain bandwidth is also an important performance of the FPC antenna. For this antenna, the 3-dB gain bandwidth is 11.9% at 4.6 GHz and 8.2% at 5.5 GHz. They are larger than the impedance bandwidth. So the impedance bandwidth is used as the working bandwidth of the proposed FPC antenna. We show the simulated and measured gains of the antenna in both states in Fig. 12. The antenna achieves maximum gain at 4.6 GHz and 5.5 GHz, respectively. The measured gain of the antenna is a little lower than the simulated one. The measured gain of the

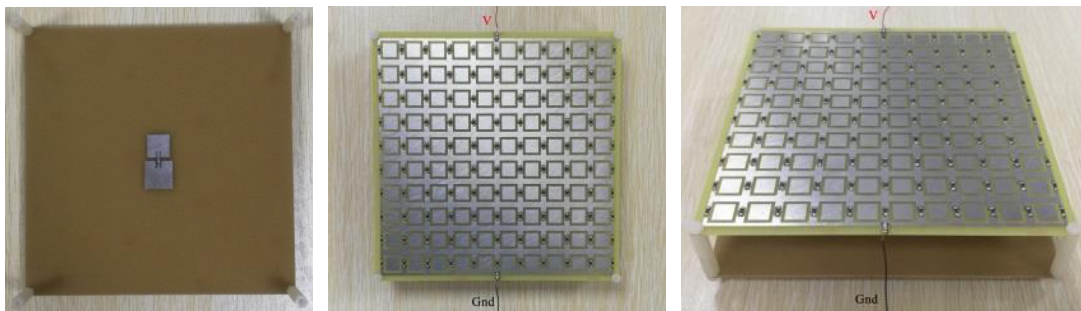


Figure 9. Photographs of the fabricated antenna.

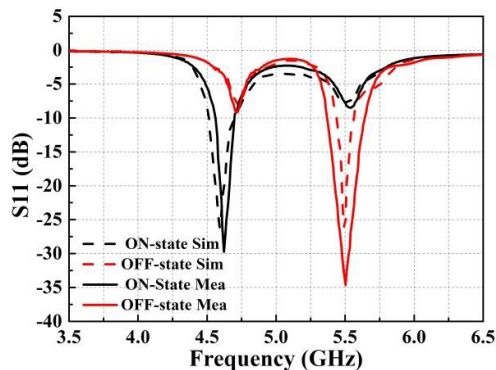
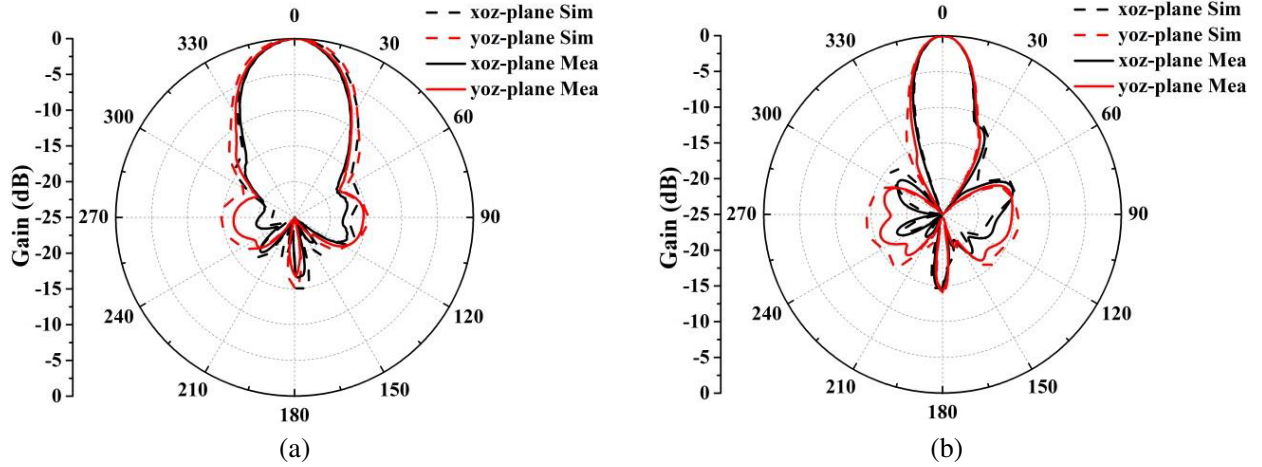
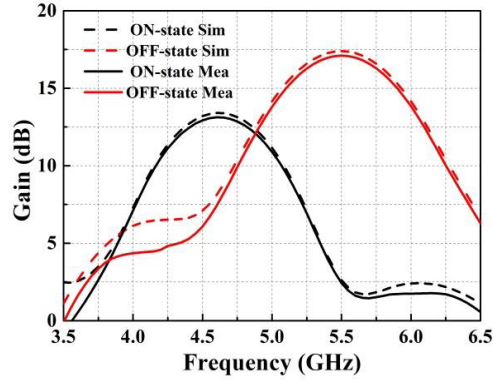


Figure 10. Simulated and measured  $S_{11}$  of the antenna.



**Figure 11.** Simulated and measured radiation patterns of the antenna. (a) 4.6 GHz in ON state; (b) 5.5 GHz in OFF state.



**Figure 12.** The gain of the antenna in both states.

**Table 1.** The comparison of the dual-band FPC antenna.

Antenna mode	Electrical size	Superstrate	Antenna character	Frequency (GHz)	Gain (dB)
Antenna in [5]	$2.5\lambda_{1.78 \text{ GHz}} \times 2.5\lambda_{1.78 \text{ GHz}}$	Metallic strip lines	Dual-band	1.71	17
				1.78	17
Antenna in [8]	$3\lambda_{5.5 \text{ GHz}} \times 3\lambda_{5.5 \text{ GHz}}$	Two layers PRSs	Dual-band	2.5	14
				5.5	14.9
Antenna in [9]	$2.6\lambda_{13 \text{ GHz}} \times 2.6\lambda_{13 \text{ GHz}}$	Single layers FSS	Dual-band	6.9	16.5
				13	20.9
Antenna in this paper	$2.5\lambda_{5.5 \text{ GHz}} \times 2.5\lambda_{5.5 \text{ GHz}}$	Single layer Reconfigurable PRS	Frequency reconfiguration	4.6	13.1
				5.5	17.1

antenna is 13.1 dB at 4.6 GHz in ON state and is 17.1 dB at 5.5 GHz in OFF state. Besides, we calculate the radiation efficiency of the antenna. The radiation efficiency of the antenna is 81.8% at 4.6 GHz and 85.5% at 5.5 GHz.

Table 1 shows the comparison of the performances of the proposed frequency reconfigurable FPC antenna and dual-band FPC antennas in [5, 8], and [9]. We note that the proposed antenna has a small electric size. And the antenna can operate at two different bands with a single-layer PRS. Besides, the operating frequency of the proposed antenna can be tuned easily.

## 5. CONCLUSION

A frequency reconfigurable FPC antenna with a single-layer PRS has been presented. A novel reconfigurable PRS with PIN diodes on it is used as the superstrate of the antenna. A dual-band patch antenna works as the radiator. Through controlling the state of the diodes, the PRS can present different reflection phases. They will make the antenna work at different frequencies. Thus, the frequency reconfiguration of the antenna is realized. The antenna is simulated and optimized by CST. A prototype antenna is fabricated and measured. The measured results agree well with the simulated ones. The proposed antenna realizes bandwidths of 4.55–4.7 GHz (3.3%) and 5.37–5.63 GHz (4.7%) with peak gains of 13.1 dB and 17.1 dB at 4.6 GHz and 5.5 GHz, respectively. Besides, this designed method proposed in this paper can also be used to design an FPC antenna working at other frequencies.

## REFERENCES

1. Yeo, J. and D. Kim, "Novel design of a high-gain and wideband Fabry-Pérot cavity antenna using a tapered AMC substrate," *J. Infrared Milli. Terahz Waves*, Vol. 30, 217–224, 2009.
2. Zeb, B. A., R. M. Hashmi, K. P. Esselle, and Y. Ge, "The use of reflection and transmission models to design wideband and dual-band Fabry-Perot cavity antennas," *2013 International Symposium on Electromagnetic Theory*, 1084–1087, 2013.
3. Kim, D., J. Ju, and J. Choi, "A broadband Fabry-Perot cavity antenna designed using an improved resonance prediction method," *Microw. Opt. Technol. Lett.*, Vol. 53, No. 5, 1065–1069, May 2011.
4. Wang, N., Q. Liu, C. Wu, L. Talbi, Q. Zeng, and J. Xu, "Wideband Fabry-Perot resonator antenna with two complementary FSS layers," *IEEE Trans. Antennas Propag.*, Vol. 62, No. 5, 2463–2471, May 2014.
5. Kim, D., "Novel dual-band Fabry-Pérot cavity antenna with low frequency separation ratio," *Microw. Opt. Technol. Lett.*, Vol. 51, No. 8, 1869–1872, August 2009.
6. Konstantinidis, K., A. P. Feresidis, and P. S. Hall, "Dual subwavelength Fabry-Perot cavities for broadband highly directive antennas," *IEEE Antennas Wirel. Propag. Lett.*, Vol. 13, 1184–1186, 2014.
7. Konstantinidis, K., A. P. Feresidis, and P. S. Hall, "Multilayer partially reflective surfaces for broadband Fabry-Perot cavity antennas," *IEEE Trans. Antennas Propag.*, Vol. 62, No. 7, 3474–3481, July 2014.
8. Abdelghani, M. L., H. Attia, and T. A. Denidni, "Dual- and wideband Fabry-Perot resonator antenna for WLAN applications," *IEEE Antennas Wirel. Propag. Lett.*, Vol. 16, 473–476, 2017.
9. Meng, F. and S. K. Sharma, "A dual-band high-gain resonant cavity antenna with a single layer superstrate," *IEEE Trans. Antennas Propag.*, Vol. 63, No. 5, 2320–2325, May 2015.
10. Vaid, S. and A. Mittal, "A low profile dual band resonant cavity antenna," *International Journal of RF and Microwave Computer-Aided Engineering*, Vol. 27, No. 2, 2017.
11. Trentini, G. V., "Partially reflecting sheet arrays," *IRE Trans. Antennas Propag.*, Vol. 4, No. 4, 666–671, Oct. 1956.